METHODS OF DETERMINATION OF CRACKING INDICATORS OF ROCKS AS A RESULT OF BLASTING

Djaksimuratov Karamatdin Mustapaevich
Candidate of Natural Sciences, Nukus Mining Institute
Dariyabaev Abumalik Temurbek o'g'li
Student of Nukus Mining Institute
Joldasbayeva Aysulu Baxitbay qizi
Student of Nukus Mining Institute
Maulenov Nurlibek Axmet o'g'li
Student of Nukus Mining Institute
https://doi.org/10.5281/zenodo.7110306

Abstract. *A blasting experiment was conducted on iron ore samples by considering multiple coupling charge coefficients. The resulting internal fracture and damage characteristics were quantitatively analyzed via computerized tomography (CT), scanning, and three-dimensional (3D) model reconstruction. The results show that the iron ore primarily displayed radial and circumferential cracks along the blast hole under an explosive load. When the decoupling coefficient was small, the crack surface was dominated by transgranular fractures in the form of intracrystalline fractures. As the uncoupling coefficient increased, the crack surface exhibited transgranular and intergranular coupled fracture modes. Using fractal theory to analyze crack distribution characteristics, as the decoupled coefficient increased, the body fractal dimension tended to decrease, and the degree of damage gradually decreased. The degree of damage reached a turning point when the decoupling charge coefficient was approximately 1.33. A numerical simulation suggested that the explosion energy transmitted to the iron ore and the effective stress decrease sharply when the decoupling coefficient exceeds 1.33. In some optimal uncoupling coefficient range, excessive fragmentation of the ore body is prevented, thereby allowing full use of the explosive energy.*

Keywords: *study combined CT scanning and 3D reconstruction to analyze the effect, passive confining pressure device and the explosive, CT scanning and 3D reconstruction of iron ore, fractal dimensions of a radial uncoupled 3D body, relationship between decoupled coefficient and blasting action.*

МЕТОДЫ ОПРЕДЕЛЕНИЯ ПОКАЗАТЕЛЕЙ ТРЕЩИНОВАТОСТИ ГОРНЫХ ПОРОД В РЕЗУЛЬТАТЕ ВЗРЫВНЫХ РАБОТ

Аннотация. *Эксперимент по взрывным работам был проведен на образцах железной руды с учетом нескольких коэффициентов заряда связи. Полученные характеристики внутренних трещин и повреждений были количественно проанализированы с помощью компьютерной томографии (КТ), сканирования и реконструкции трехмерной (3D) модели. Результаты показывают, что железная руда в основном имеет радиальные и кольцевые трещины вдоль шпура под взрывной нагрузкой. При малом коэффициенте развязки на поверхности трещин преобладали трансзерновые изломы в виде внутрикристаллитных изломов. По мере увеличения коэффициента разобщения поверхность трещины демонстрировала транскристаллитные и межкристаллитные режимы связанного разрушения. Используя теорию фракталов для анализа характеристик распределения трещин, по мере увеличения коэффициента развязки фрактальная размерность тела имела тенденцию к уменьшению, а степень* *повреждения постепенно уменьшалась. Степень повреждения достигла критической точки, когда коэффициент развязывающего заряда составил примерно 1,33. Численное моделирование показало, что энергия взрыва, передаваемая железной руде, и эффективное напряжение резко уменьшаются, когда коэффициент развязки превышает 1,33. В некотором оптимальном диапазоне коэффициентов разобщения предотвращается чрезмерное дробление рудного тела, что позволяет полностью использовать энергию взрыва.*

Ключевые слова: *исследование комбинированного КТ-сканирования и 3D-реконструкции для анализа воздействия, пассивное всепоглощающее устройство давления и взрывчатое вещество, КТ-сканирование и 3D-реконструкция железной руды, фрактальные размерности радиально-несвязанного 3D-тела, взаимосвязь между коэффициентом развязки и действием взрыва.*

INTRODUCTION

Iron ore, a raw material used in steel manufacturing, is typically mined by blasting. The energy utilization rate of explosives can be increased, and the energy consumption rate of blasting equipment decreased, by adopting a rational decoupled charge approach . During mining, the lumpiness of the iron ore should be neither too large nor too small . This balance requires a rational and accurate determination of the decoupling charge coefficients. Most scholars used numerical simulation to study the explosion stress distribution characteristics of uncoupled charge, and fitted the propagation curve of effective stress . Results of dynamic caustic experiments and the digital image correlation test method have enabled the identification of the mechanism of crack interconnection during concentric decoupled charge. They also determined the crack growth rate, the stress intensity factor, and the crack growth energy release rate, and obtained the law of full-field strain attenuation under uncoupled charge . Using the model experiment method, combined with fractal damage theory and energy release rate theory, it has been possible to study fractal damage in the breakage zone, the fracture zone, and the crush zone in coupled and decoupled charge blasting (using air and clay as the filling medium, respectively). The energy release rate of a blast-induced crack was also analyzed . When using expandable polystyrene foam as the filling medium, the radius, depth, and volume of the blasting funnel of a model specimen are greater, the flyrock launch velocity is slower, the peak stress in the specimen is higher, and the distribution of gravel lumpiness is even greater . The combination of X-ray computerized tomography (CT) and three-dimensional (3D) reconstruction is effective for nondestructively visualizing and collecting quantitative data on the structural characteristics of coal . Tensor parameters can be derived from these 3D reconstructions to provide data on crack initiation . A quantitative evaluation of the law of damage development assesses the following effects: crack development on rock strength, the loading force on the crack distribution, and temperature and stress on crack development and pore structures . This study combined CT scanning and 3D reconstruction to analyze the effect of the explosion load on crack propagation in iron ore. Fractal theory is commonly used to analyze failure in discontinuous media. The gray correlation coefficient is used to determine crack locations in coal and rock The perspective adopted in most of the studies cited above considered the stress and strain field in uncoupled charge explosions, and did not reveal the effect of uncoupled charge on the distribution of the 3D explosion fracture field in the medium. In contrast, this study conducted a CT scanning experiment on iron ores subjected to blasting with different uncoupling charge coefficients. 3D digital image processing and 3D model reconstruction were applied to analyze post-explosion fractures within the iron ore. The distribution characteristics of the internal cracks were observed, and the interior damage was analyzed horizontally to determine the failure mechanism of the iron ore. We hence propose a method for characterizing the internal damage of iron ores. We discuss the damage law of the ore relative to the uncoupling charge coefficients, and establish the relationships between the degree of damage and uncoupling charge coefficients. In addition, we analyze the energy transfer and effective stress of explosives under uncoupled charges using numerical calculations. Our results provide a theoretical basis for the structural optimization and design of blast charges in the context of iron-ore mining applications.

MATERIALS AND MAETHODS

Effects of uncoupled charging on the iron ore failure law

The iron ore sample was placed in a passive confining pressure device with an inner diameter of 50 mm, as shown in Figs. 4a–c. The passive confining pressure device has an inner and outer layer. The outer layer has a flange design, and the inner layer is a container that accommodates the test pieces. A flange cover was

tightened over the upper part after the test piece was properly arranged in the container; its purpose is to ensure the structure integrity of iron ore in subsequent CT scan experiments. When the iron ore is placed in a passive confining pressure device, plastic material is wound around the iron ore, on the one hand to minimize the effect of boundary reflections, on the other hand to ensure that there is no gap between the iron ore and the device. The explosive used in this case was dinitrodiazophenol (DDNP) with a charged mass of 150 mg, a charging height of 4 cm, and a blocking height of 3 cm. In order to ensure the uncoupled charge, the explosive can be located in the center of the blast-hole, and tetrafluorine gaskets of different diameters are placed on both ends of the explosive to form the uncoupled charge pack, as shown in Fig. 4d. Fine sand served as the blocking material. The explosive was detonated using a high-voltage discharge Iron ore fracture surface under uncoupled charging Post-explosion iron-ore results are shown in Fig. 5. No significant fracture cracks occurred in the ore when the decoupling coefficient was 3.00 or 3.33. The initial pressure produced by the explosion in the blast hole did not cause failure when the decoupling coefficient was high. The distribution of the explosive cracks was random when the decoupling charge coefficient was between 1.00 and 2.67. Under different charging structure conditions, the crack distribution exhibited specific statistical characteristics. The number of cracks on the top surface of the test piece first increases and then decreases as the decoupling charging coefficient increases. The maximum number of cracks occurs when the decoupling coefficient is 1.33. When the ore is subjected to an explosive load, the decoupling charge coefficient affects the fracture behavior. Most fractures are manifested as radial and ring fracture cracks along the blast-hole direction. The radial cracks move outward from the blast-hole center when the circumferential tensile stress exceeds the ultimate dynamic tensile strength of the medium. Ring cracks occur when the medium is subjected to a radial tensile stress. Transgranular (TG) and intergranular (IG) fractures are the two main forms of destruction between the grains. Xie and Chen noted that TG destruction dissipates more energy than IG destruction. Scanning electron microscopy (SEM) images of the blasted iron ore with decoupling coefficients 1.33 and 2.67 are shown in Fig. 6. After iron-ore blasting, the iron ore was cut to the required size in the target area of the crack surface of interest. Because iron ore is a conductive substance, there is no need to spray its surface with conductive material. When the decoupling coefficient is small, the strong impact of the explosive stress wave and detonation gas causes shear brittle failure in the ore body. Cracks penetrate the crystals and the crack surface is dominated by TG fractures in the form of intracrystalline fractures. The crack

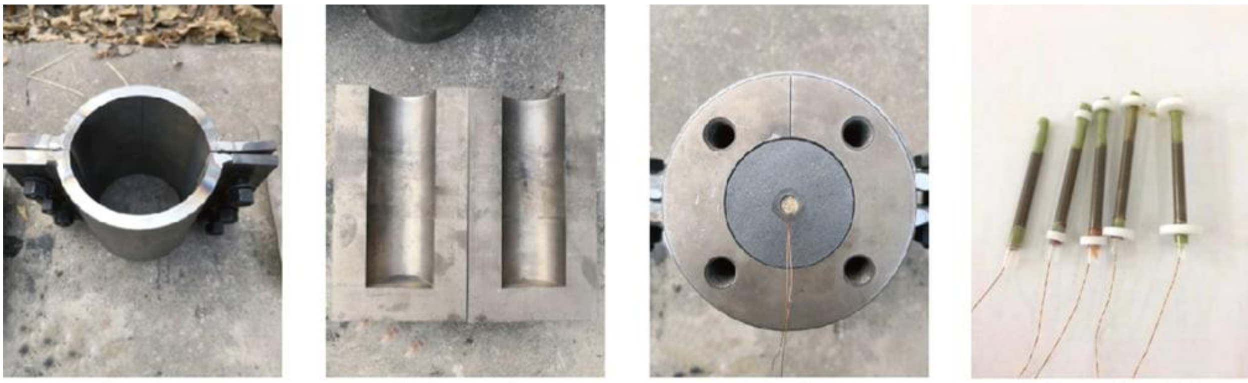

(a) Outer flange (b) Liner container (c) Top flange (d) Uncoupled explosive

Fig. 4. Passive confining pressure device and the explosive.

Fig. 5. Blasted iron ore under different decoupling charge coefficients.

surface is relatively flat and smooth. When the uncoupling coefficient increases, the explosion energy becomes attenuated in the air layer, and the peak value of the initial explosion shock wave incident on the borehole wall decreases. This shows TG and IG coupled fracture modes in the iron ore. The crack surface becomes more tortuous.

RESULTS

CT scanning and 3D reconstruction of iron ore

CT scanning reveals internal changes in the material in response to force . CT scanning was performed at the National Key Laboratory of Coal Resources and Safe Mining, of the China University of Mining and Technology - Beijing, using apparatus No. ACTIS300–320/225, as shown in Fig. 7. The scanning voltage was 280 kV and the scanned sections of the test pieces were 0.0– 100.0 mm. One layer was scanned every 0.1 mm to produce a total of 1000 images. Threshold segmentation is a simple and frequently used method for segmenting digital images. In this study, each image was processed using multithreshold segmentation by selecting a gray threshold that distinguished iron ore and cracks. The original CT image was converted to an image comprising only two grey levels. Fig. 8 shows a processing chart of the scanned image and the gray threshold for the uncoupling coefficients n=1.00, 1.33, and 2.67, where the cracks are observable. Gray represents iron ore and the white regions represent the cracks formed post-explosion. A 3D reconstruction can reflect some of the internal cracks of the coal and rock mass . Fig. 9 shows the 3D distribution of fissures in several iron ore samples. The results of gray threshold processing were used to create 3D reconstructions of the test pieces for different coupling coefficients. The number of internal cracked surfaces in the test piece decreases as the decoupling coefficient increases. When n=1.00, most cracks are radial and penetrate the entire test piece, and circumferential cracks are formed

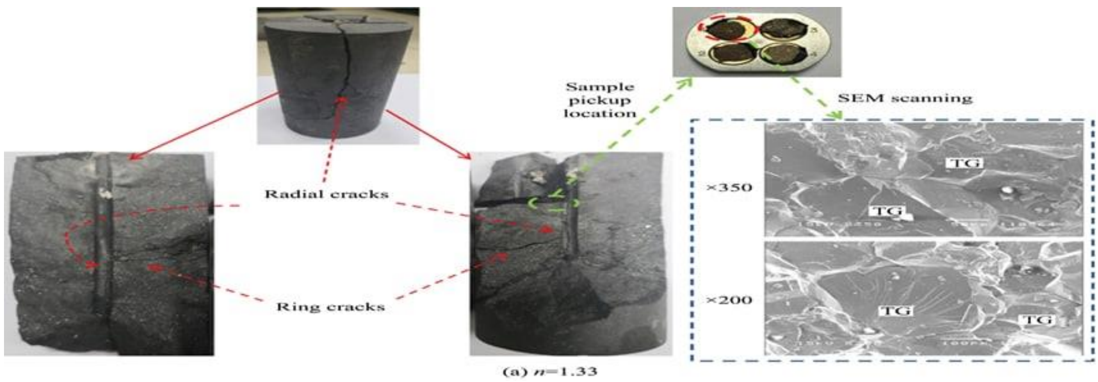

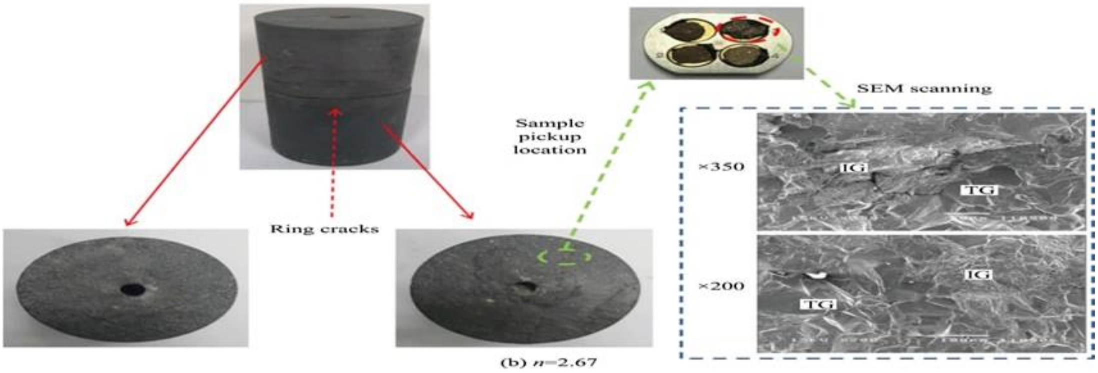

Fig. 6. Cracks in the iron ore surface.

The formation of these two types of crack surfaces is attributable to the excessive attenuation of explosive energy in the air layer and to the resulting decrease in energy acting on the medium. In addition, the iron ore undergoes brittle failure in most cases. The cracks propagate along the blast hole wall, as observed in the reconstructed images. The formation of explosive cracks within the iron ore is closely associated with the charging decoupling coefficient. In engineering practice, if the blast-hole decoupling coefficient is excessively large, fewer explosive cracks occur in the ore body, and ore lumps are more likely to occur. This is disadvantageous for subsequent ore processing.

Fractal dimensions of a radial uncoupled 3D body

Fractal theory is commonly used to analyze failure in a discontinuous medium. Fissures form when the medium fails, when subjected to an explosive load. The degree of damage within the rock can be characterized in terms of the fractal dimension . The degree of damage to the material and the fractal dimension D are related as.

$$\omega = \frac{D_t - D_0}{D_t^{max} - D_0}$$

where Dt denotes the fractal dimension of the area of damage to the medium; D0 the fractal dimension of the damage in the medium before the explosion; Dmax t the fractal dimension when the area of damage to the medium is maximal, Dmax t ¼2 for a 2D problem and Dmax t ¼3 for a 3D problem. The calculated fractal dimensions of the iron ore under uncoupled charging are shown in Fig. 10. When the uncoupled charging coefficients are 1.00, 1.33, 1.67, 2.00, 2.33, and 2.67, the corresponding fractal dimensions of the 3D body are 2.5112, 2.4659, 2.0925, 1.8224, 1.7296, and 1.5524, respectively. The degrees of damage (x) to the samples per fractal dimension of the 3D iron-ore body are 0.8371, 0.8220, 0.6575, 0.6075, 0.5765, and 0.5175 for uncoupled charging values when n is 1.00, 1.33, 1.67, 2.00, 2.33, and 2.67, respectively. The relationship between the decoupling coefficient and x is shown in Fig. 11. Uncoupled charging produces an air interlayer between the charge and the blast-hole wall. This buffer decreases the effect of the explosive stress wave and prolongs the time during which the detonation gas is active, thereby allowing the cracks to propagate fully. In this experiment, when the decoupling coefficient was small, the detonation wave initially affected the air interlayer; the detonation wave transformed into an air shock wave and then acted on the blast-hole wall. The air shock wave attenuated rapidly as the decoupling coefficient increased. The appropriate energy attenuated even faster, and the degree of damage steadily decreased. When the decoupling coefficient n was 1.33, the curve dropped suddenly. This change indicates the existence of an ‘‘optimal uncoupling coefficient range”. When n is within this range, the fragmentation of the iron ore is optimal.

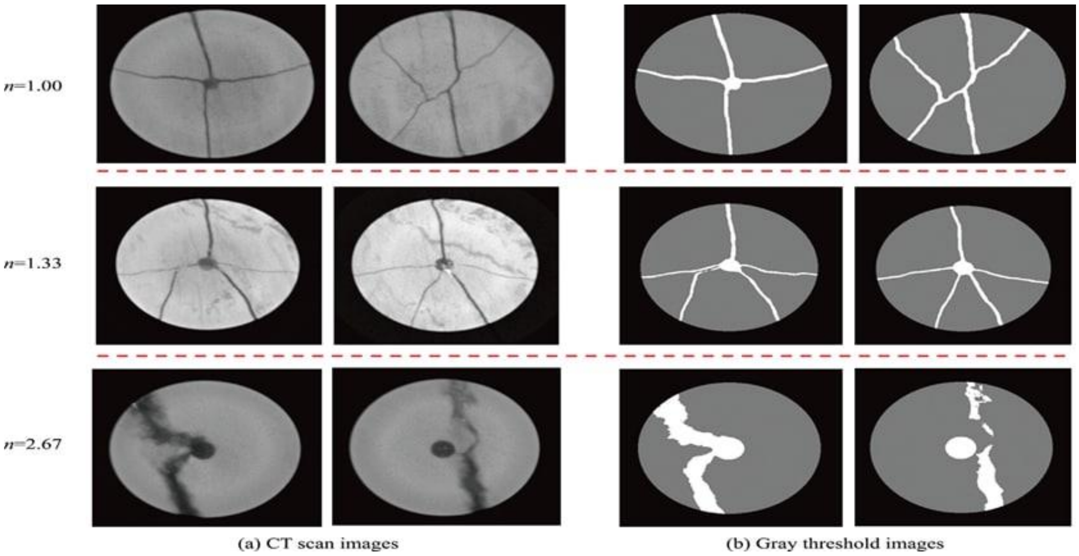

Fig. 8. Scanned image of an iron ore test piece and the image after gray threshold processing

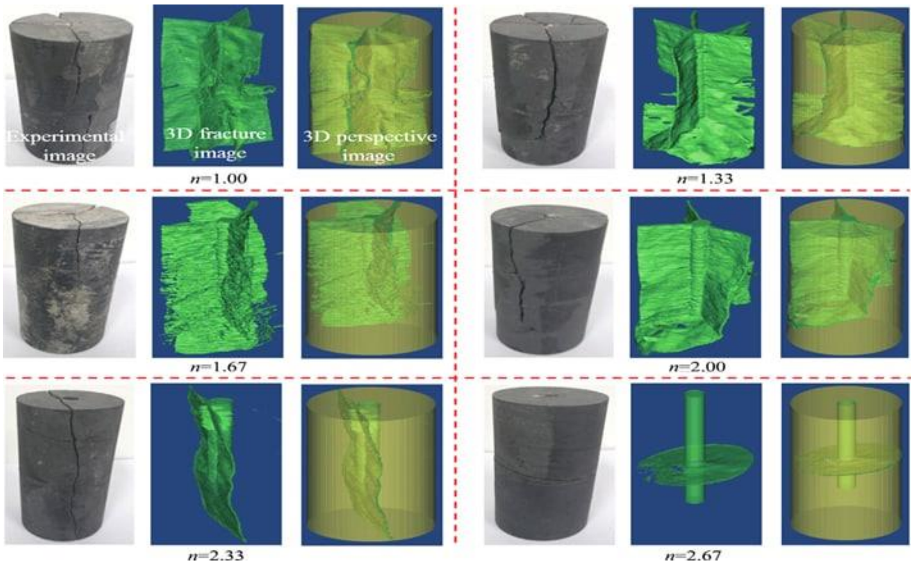

Fig. 9. 3D distribution of cracks in iron ore samples.

DISCUSSION

Relationship between decoupled coefficient and blasting action

Accordingly, a two-dimensional numerical calculation model was established, as shown in Fig. 12. The outer diameter of the proposed model was 50 mm and the diameter of the explosive was 3 mm. Six blast-hole diameters consistent with those in the study were set up, corresponding to the six decoupled coefficients used in the experiment. Blue, yellow, and green represent iron ore, air and the explosives, respectively. Fig. 13 illustrates the propagation process of the Von Mises stress wave in the iron ore (n=1.67). Throughout the numerical calculation, in the case of a decoupled charge, the detonation wave formed by the explosion first acts on the air in the gap between the charge and the blast hole, thereby generating an air blast wave. This wave propagates in the gap and encounters the blast-hole wall, generating an impact pressure. Depending on the charge structure, the initial pressure generated by the explosion on the blasthole wall is also different. Fig. 14 shows the time history curve of the explosive energy under uncoupled charge. When the explosive is used to blast the iron ore medium, the difference in the explosion energy transfer increases as the uncoupling coefficient increases. The difference of explosion energy transfer between different coupling media is not constant. When the uncoupling coefficient is small, the difference of explosion energy transfer is small. When it is large, the difference of explosion energy transfer is also large. When the decoupling coefficient is less than or equal to 1.33, the explosion energy is transferred more to the iron ore, resulting in the effective formation and crushing of the iron ore. However, when the decoupling coefficient exceeds 1.33, less explosion energy transferred to iron ore, which cannot be effectively crushed. The stress on the iron core varies with the decoupling coefficients. According to different calculation models, the first monitoring point was selected at a distance of 3 mm from the blast-hole wall, and the remaining 7 measuring points were separated by equal intervals of 3 mm, as shown in Fig. 12. The time-history curve of the effective stress propagation was extracted to obtain the stress peak point for different coupling coefficients, as shown in Fig. 15. In the case of uncoupled charges, the effective stress decreases exponentially with the ranging. For iron-ore blasting, in the case of a decoupled charge, the stress wave changes significantly, and the peak value of the stress wave decreases as the decoupled coefficient increases. This curve indicates that, in the

CONCLUSIONS

Damage to iron-ore samples under explosive loading is predominantly radial, and circumferential cracks form the blast-hole direction. When the decoupling coefficient increases, the crack transforms from radial to circumferential

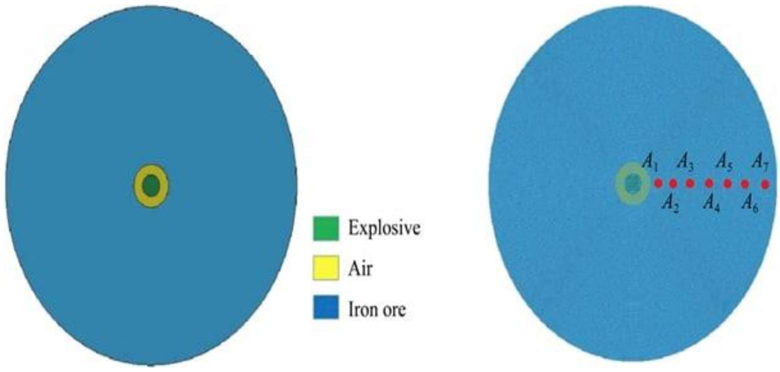

Fig. 12. Calculation model.

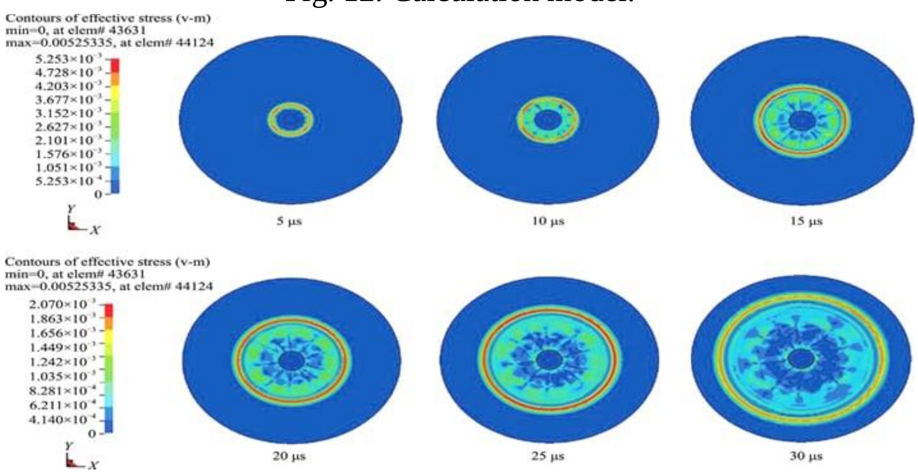

Fig. 13. Propagation of Von Mises stress wave and crack progagation (n=1.67).

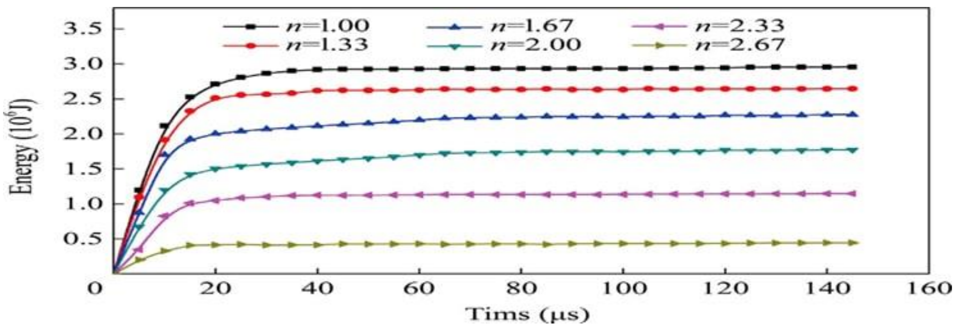

Fig. 14. Time history curve of explosion energy under uncoupled charge.

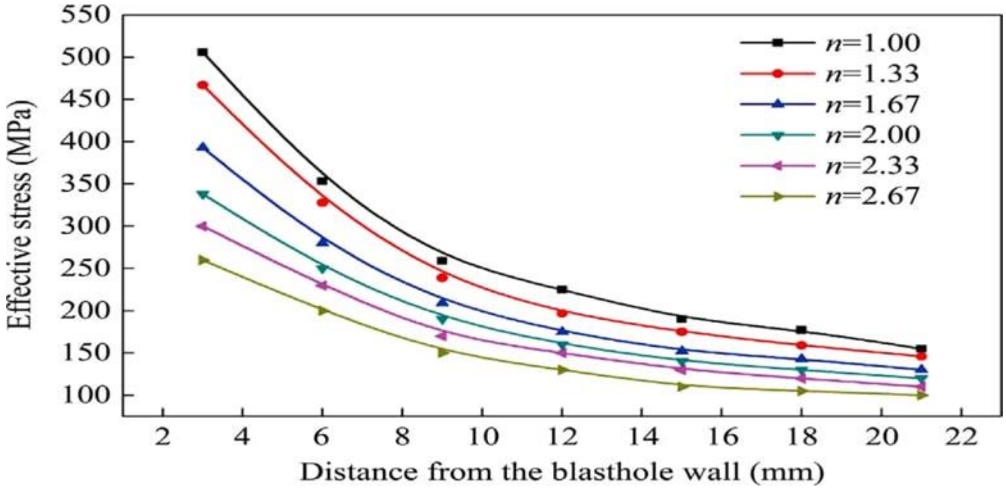

Fig. 15. Relationship between effective stress peak value and distance of uncoupled charge

When the decoupling coefficient is small, the crack surface is dominated by transgranular fractures in the form of intracrystalline fractures. As the uncoupling coefficient increases, the crack surface exhibits transgranular and intergranular coupled fracture modes. As the decoupled coefficient increases, the body fractal dimension tends to decrease, and the damage degree gradually decreases. The relationship between the decoupling charge coefficient and the degree of damage was determined to contain an attenuation region when the decoupling coefficient was approximately 1.33. When the decoupling coefficient exceeds 1.33, the explosion energy transmitted to the iron ore through the air layer decreases sharply, and the effective stress generated also decreases. There is an ‘‘optimal uncoupling coefficient range” that can be exploited to prevent excessive fragmentation of the ore body, thereby achieving optimal fragmentation effects.

REFERENCES

1. Jones T, Nordlund E, Wettainen T. Mining-induced deformation in the malmberget mine. Rock Mech Rock Eng 2019;52(6):1903–16.
2. Ye L, Peng ZW, Wang LC, Anzulevich A, Bychkov I, Tang HM, Rao MJ, Zhang YB, Li GG, Jiang T. Preparation of core-shell iron ore-biochar composite pellets for microwave reduction. Powder Technol 2018;338:365–75.
3. Xu S, Liang RY, Suorineni FT, Li YH. Evaluation of the use of sublevel open stoping in the mining of moderately dipping medium-thick orebodies. Int J Min Sci Technol 2021;31(2):333–46.
4. Zhang T, Yu LY, Su HJ, Zhang Q, Chai SB. Experimental and numerical investigations on the tensile mechanical behavior of marbles containing dynamic damage. Int J Min Sci Technol 2022;32(1):89–102.
5. Silva J, Worsey T, Lusk B. Practical assessment of rock damage due to blasting. Int J Min Sci Technol 2019;29(3):375–85.
6. Wang W, Zhang JQ, Liu A. Study on eccentric uncoupled blasting effect of cutting seam pipe. Coatings 2021;11(1):104.
7. Chen M, Ye ZW, Lu WB, Wei D, Yan P. An improved method for calculating the peak explosion pressure on the borehole wall in decoupling charge blasting. Int J Impact Eng 2020;146:103695.
8. Guo ZW, Huang GY, Zhu W, Liu H, Feng SS. Mechanism and suppression of the effect of axial rarefaction waves on the eccentric initiation effect. Int J Impact Eng 2019;124:37–47.
9. Wang YB. Study of the dynamic fracture effect using slotted cartridge decoupling charge blasting. Int J Rock Mech Min Sci 2017;96:34–46.
10. Guo DM, Liu K, Lu H, Yang RS, Wang CL, Wang YB. Fracture behavior of an empty hole using the digital laser dynamic caustic method under directional controlled blasting. Mater Test 2016;58(11–12):982–91.
11. Yang RS, Ding CX, Yang LY, Lei Z, Zheng CD. Study of decoupled charge blasting based on high-speed digital image correlation method. Tunn Undergr Space Technol 2019;83:51–9.
12. Ding CX, Yang RS, Lei Z, Wang M, Zhao Y, Lin H. Fractal damage and crack propagation in decoupled charge blasting. Soil Dyn Earthq Eng 2021;141:106503.
13. Zhang YP, Luo Y, Wan SP, Tian YX, Ding HC, Zhang XX. Influence of decoupled charge structure and filler on the blasting effect. Shock Vib 2020;2020:1–13.
14. Yu SF, Wu AX, Wang YM. Insight into the structural evolution of porous and fractured media by forced aeration during heap leaching. Int J Min Sci Technol 2019;29(5):803–7.